Biochemical and Biophysical Research Communications **289,** 97–102 (2001)
doi:10.1006/bbrc.2001.5964, available online at http://www.idealibrary.com on IDEAL®

Boundary Sequences of the NADPH Oxidase p67^{phox} C-Terminal SH3 Domain Play on Its Specificity

Shen-Long Hwang,* Tai-Shan Cheng,† Chang-Han Chen,† Yuh-Ju Sun,‡ Chwan-Deng Hsiao,‡ and Yi-Ren Hong†,[1]

**Neurosurgery Department and †Graduate Institute of Biochemistry, Kaohsiung Medical University, Kaohsiung, Taiwan, Republic of China; and ‡Institute of Molecular Biology, Academia Sinica, Taipei, Taiwan, Republic of China*

Received October 18, 2001

SH3 domains are found in many signal transduction proteins where they mediate protein–protein binding by recognizing specific peptides rich in proline. Based on the analysis of sequence alignment data, the NADPH oxidase p67^{phox} C-terminal SH3 domain possesses a typical compact β-barrel consisting of five β-strands arranged in two antiparallel β-sheets of three and two β-strands. Multiple amino acid substitutions were made at βe and its flanking residues to determine the role of the boundary sequences in binding activity and conformational specificity of the domain. Analysis of amino acid P55 indicated that all mutants were completely abolished in their binding activities. The substitution of F58 with Y58 showed no effect of the binding, whereas substitution with stop codon abolished activity. Furthermore, when amino acid V59 was substituted with stop codon, activity was also completely abolished. Substitution of E60 with stop codon showed no effect of binding. Moreover, our data show that V59 particularly could not be replaced by Leu. Taken together, these data suggest that V59 may not only contribute the exact boundary site but also play on the specificity for protein–protein interactions in phagocyte NADPH oxidase.

Superoxide is generated by a phagocyte NADPH oxidase which is assembled as a complex of at least four proteins localized to plasma and phagolysosomal membranes (1). Cytochrome b_{558}, an integral membrane flavoprotein composed of two subunits of 91 and 22 kDa (gp91^{phox} and p22^{phox}), is the oxidase protein responsible for transferring electrons from NADPH to O_2 (2). p47^{phox}, p67^{phox}, p40^{phox}, and *rac* are found in the cytosol of resting neutrophils (3–5). There is abundant evidence that p47^{phox} binds to p67^{phox} *in vitro* (6–14). p47^{phox}, p67^{phox}, p40^{phox}, and p22^{phox} each contain peptides that conform to proposed consensus sequences for proline-rich peptides bound by SH3 domains (4–7). p47^{phox} and p67^{phox} each contain two peptide domains of ~60 amino acids which share homology with SH3 domains (15). Existence of SH3 domains and proline-rich peptide sequences in p47^{phox} and p67^{phox} suggested that these specialized regions may facilitate binding between the two proteins. We previously studied the interactions between p47^{phox} and p67^{phox} under intracellular conditions using the yeast two-hybrid/interaction trap assay for protein–protein binding. We found the interaction between p67^{phox} C-terminal SH3 domain (residues 453–516, renumber 1–64, Fig. 1) and p47^{phox} proline-rich region (362–370, QPAVPPRPS) (unpublished data).

The X-ray crystal or NMR structure of SH3 domain is shown to be a compact β barrel consisting of five β-strands arranged in two antiparallel β-sheets of three and two β-strands (16–19). The C-terminal SH3 domain of p67^{phox} binds to its natural ligand was modeled using the *c-abl* SH3 domain structure as a template (17). Though the SH3 domain and its target proline-rich region have been determined, sequences that determine the exact boundary of biological behavior of SH3 domain and its target proline-rich region are still unknown. To gain insight into the role of the boundary sequences of the SH3 domain βe and its flanking residues involved in binding activity, we performed site-directed and random mutagenesis combining the yeast two-hybrid method to determine the boundary sequence in p67^{phox} C-terminal SH3 domain. Our data suggest that V59 provides not only the boundary site, but also the critical site for maintaining the βe portion in the β-barrel structure of SH3 domain.

Abbreviations: SH3, *src* homology 3; ONPG, *o*-nitrophenyl β-D-galactopyranoside; X-gal, 5-bromo-4-chloro-3-indolyl-β-D-galactopyranoside; TRP, tryptophan; URA, uracil; HIS, histidine; LEU, leucine; BCIP, 5-bromo-4-chloro-3-indolyl phosphate; NBT, nitroblue tetrazolium; bd, binding domain; ad, activation domain.

[1] To whom correspondence and reprint requests should be addressed at Graduate Institute of Biochemistry, Kaohsiung Medical University, No. 100, Shih-Chuan 1st Road, Kaohsiung 80708 Taiwan, Republic of China. Fax: 886-7-3218309. E-mail: m835016@cc.kmu.edu.tw.

0006-291X/01 $35.00

Furthermore, our data show that V59 particularly could not be replaced by Leu, suggesting that this residue may also participate in the specificity of SH3 interactions in phagocyte NADPH oxidase.

MATERIALS AND METHODS

Plasmids. Parent plasmids containing full-length $p47^{phox}$ and $p67^{phox}$ cDNA were gifts of Harry Malech and Thomas Leto (Laboratory of Host Defenses, NIAID, NIH, Bethesda, MD). pEG202, pJG4-5, and pSH18-34 shuttle vector plasmids and EGY48 strain *Saccharomyces cerevisiae* were gifts of Jenó Gyuris, Erica Golemis, and Roger Brent (Massachusetts General Hospital, Boston, MA) (20). $p40^{phox}$ SH3, $p47^{phox}$ N-terminal SH3 domains, $p47^{phox}$ and $p67^{phox}$-proline rich domains were gifts from Michael E. Kleinberg (University of Maryland, MD). Plasmids were propagated in *Escherichia coli* in LB broth containing ampicillin.

Site-directed mutagenesis and random mutagenesis. To perform either site-directed mutagenesis or random mutagenesis on βe and flanking sequences (P55, F58, V59 and E60 of the $p67^{phox}$ C-terminal SH3 domain). Primers designed for site-directed mutagenesis: sense primer, 5′-CG**GAATTC**GGCAGCGAAGTGGAG-3′; anti-sense primers are 5′-ACGC**GTCGAC**TGTAGTTGCGCAGTCTTCAACAAA-AACTTTTTAGAAAATGCC-3′ (change P55, CCC to TAA); 5′-ACGC**GTCGAC**TGTAGTTGCGCAGTCTTCAACTTAAACTTTG-GGGAAAAT-3′ (change F58, TTT to TAA), 5′-ACGC**GTCGAC**-TGTAGTTGCGCAGTCTTCCTAAAAAACTTTGGGGAAAAT-3′ (change V59, GTT to TAG) and 5′-ACGC**GTCGAC**TGTAGTTGC-GCAGTCCTAAACAAAAACTTTGGGGAAAAT-3′ (change E60, GAA to TAG). Primers designed for random mutagenesis 5′-ACGC-**GTCGAC**TGTAGTTGCGCAGTCTTCAACAAAAACTTTNNNGAA-AATGCC-3′ (change P55, CCC to NNN); 5′-ACGC**GTCGAC**TGT-AGTTGCGCAGTCTTCAACNTAAACTTTGGGGAAAAT-3′ (change F58, TTT to TAN), 5′-ACGC**GTCGAC**TGTAGTTGCGCAGTCTTC-NNNAAAAACTTTGGGGAAAAT-3′ (change V59, GTT to NNN). Revertant was carried out with wild type sequence 5′-ACGC**GTCGAC**-TGTAGTTGCGCAGTCTTCAACAAAAACTTTGGGGAAAAT-3′ (change V59L back to V59, CTT to GTT).

Primers designed for site-directed mutagenesis of $p40^{phox}$ SH3 domain: sense primer, 5′-CG**GAATTC**ATGGCAGCTCCGAGAGCA-GAG-3′; anti-sense primers: 5′-ACGC**GTCGAC**AGGGAAGTCTTT-GAGGATCTTCTAGAAGGAGAGAGG-3′ (change V59, GTG to TAG); 5′-ACGC**GTCGAC**AGGGAAGTCTTTGAGGATCTACACGAAGGAG-AGAGG-3′ (change K60, AAG, to TAG). Primers designed for site-directed mutagenesis of $p47^{phox}$ N-terminal SH3 domain: sense primer, 5′-CG**GAATTC**ATCACCGGCCCCATCATC-3′; anti-sense primers: 5′-ACGC**GTCGAC**AGGACTGTCCAGGGGCTCCTAGAAGGACGC-TGGGATCCA-3′ (change L59, TTG to TAG); 5′-ACGC**GTCGAC**AG-GACTGTCCAGGGGCTACAAGAAGGACGCTGGGATCCA-3′ (change E60, GAG to TAG); 5′-ACGC**GTCGAC**CGTCTCGTCAGGACT-CTACAGGGGCTCGAGGAAGGACGC-3′ (change D63, GAC to ATG). Bold indicates *Eco*RI or *Sal*I restriction site. Underlined is a mutagenesis site. The PCR mixture containing 10 mM Tris–HCl (pH 8.3), 1.5 mM $MgCl_2$, 50 mM KCl, 200 mM dNTP and 2 μM of each primer with 1 unit of *Taq* polymerase was carried out by 38 cycles of 94°C for 1 min, 55°C for 1 min, and 72°C for 2 min.

DNA sequencing. All mutants were sequenced to ensure that the mutagenesis was successful. Nucleotide sequencing was performed by dideoxy method (Sequenase, USB) or ABI PRISMTM 310 genetic analyzer (Perkin–Elmer).

Detection of protein–protein interactions (21). Yeast transformed with pairs of LEXA and B42 constructs were assessed for their ability to grow in leucine-deficient galactose-containing media. Prototrophy in galactose-containing leucine-deficient media indicated reconstitution of transactivator function through $p67^{phox}$/$p47^{phox}$ binding. Yeast transformed with pairs of $p67^{phox}$/LEXA binding domain and $p47^{phox}$/B42 activation domain constructs were also scored for their ability to transactivate LexA-dependent *lacZ* gene transcription from the pSH18-34 plasmid. β-Galactosidase activity was measured by hydrolysis of X-gal on solid agar and of ONPG in two ways. First, colonies on agar plates were replicate transferred to paper soaked in Z buffer (0.15 M sodium phosphate, 10 mM KCl, 1 mM $MgSO_4$, pH 7.0) containing 0.3 mg/ml X-gal and incubated at 30°C for 30–120 min. Yeast was then lysed by dipping the paper in liquid nitrogen. Protein–protein binding was indicated by the development of blue color in lifts from colonies grown on galactose-containing agar plates. Second, yeast cotransformed with pairs of $p47^{phox} \times p67^{phox}$ fusion constructs were grown for 3–5 days in galactose-containing HIS-, URA-, and TRP-broth media to an $OD_{600\ nm}$ of 0.6–0.8. Yeast culture (1.5 ml) was pelleted and resuspended in 100 μl 0.1 M Tris buffer containing 0.1% Triton X-100. Cells were broken with multiple freeze/thaw cycles. Seven hundred microliters of Z buffer containing ONPG (final concentration 0.6 mg/ml) was added to the soluble fraction and incubated at 30°C for 30–60 min. ONPG hydrolysis was monitored by changes in $OD_{405\ nm}$ measured in a microplate reader (Thermomax, Molecular Devices, Menlo Park CA). Results were expressed as $OD_{405\ nm}/OD_{600\ nm}$ to correct for slight differences in amounts of yeast in different samples. Individual ONPG experiments were performed with duplicate samples. Yeast transformation experiments were performed at least three times.

Immunoblotting. Expression of LexA and B42 fusion proteins in yeast were detected by immunoblotting with anti-$p47^{phox}$ or anti-$p67^{phox}$ goat antisera (a gift from Harry Malech and Thomas Leto, NIAID, NIH) (20) or a monoclonal antibody against LexA from Clontech. Yeast transformed with pairs of LexA and B42 constructs were grown in log phase in glucose TRP- URA- HIS- and galactose TRP- URA- HIS- LEU- broth media at 30°C. Yeast was incubated with 5 mM diisopropyl fluorophosphate to inhibit proteases. 5-10 ml aliquots were centrifuged, extracted with SDS–PAGE sample buffer for 5 min, heated to 100°C for 2 min, and centrifuged to pellet cellular debris. Supernatant proteins were separated on SDS–PAGE gels, transferred to nitrocellulose, and immunoblotted as described (22). Polyclonal antisera were used at 1:1000 titer and the monoclonal antibody culture supernatant was used at 1:100 titer. Bands were visualized with BCIP/NBT as chromagen.

Modeling of the SH3 domain. Structure refinement and model building were carried out using the XPLOR (23). Graphics were produced using Molscript (24).

RESULTS AND DISCUSSION

Determining the Boundary Sequence of $p67^{phox}$ C-Terminal SH3 Domain: Site-Directed Mutagenesis

Figure 1 shows that the alignment of amino acid sequences of c-*src* with five SH3 domains from NADPH oxidase system. To determine the boundary sequence of $p67^{phox}$ C-terminal SH3 domain, we first performed site-directed mutagenesis at position P55, F58, V59 and E60 of the conserve region (Fig. 1). The results show that P55, F58 and V59 produced stop codon, resulting in the complete abolition of the binding to $p47^{phox}$ proline-rich region, whereas the amino acid E60 being replaced by stop codon showed no effect of binding, suggesting that this residue may not participate in

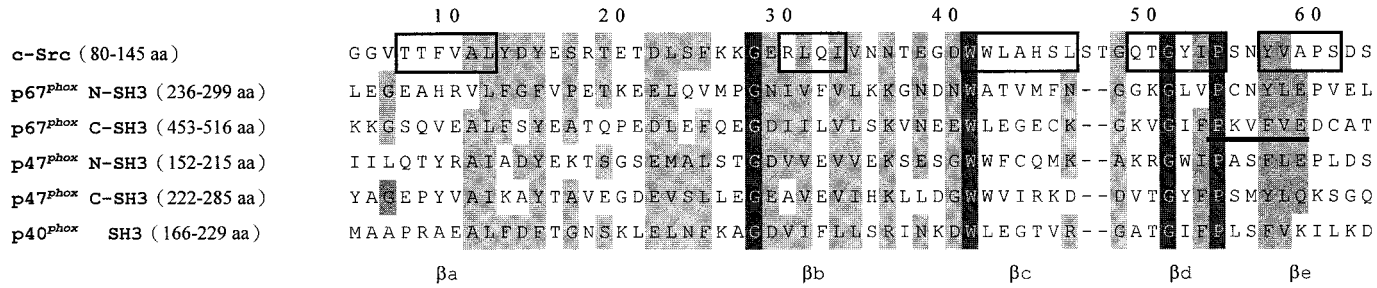

FIG. 1. Alignment of the amino acid sequences of c-*src*, p67^{phox} N, p67^{phox} C, p47^{phox} N, p47^{phox} C, and P40^{phox} SH3 domains. The positions of the five β-strands are indicated by box. βe and its flanking residues involved in mutagenesis are underlined. A black background indicates identical amino acids and a gray background indicates conserve amino acids.

βe strand (Table 1). The results clearly show that boundary site of p67^{phox} C-terminal SH3 domain is located at V59 (Table 1). Figure 2 shows that tested mutants in the yeast two-hybrid system (Fig. 2A) and all constructs were expressed equally in fusion protein level in the yeast by Western blotting (Fig. 2B).

Comparison of Other SH3 Domains in NADPH Oxidase

To further examine whether a similarity exists in all SH3 domains of NADPH oxidase, we examined two other SH3 domains which include p40^{phox} and p47^{phox} N-terminal SH3 domains. Data show that p40^{phox} exhibits a similar boundary sequence compared to p67^{phox} C-terminal SH3 domain, whereas P47^{phox} N-terminal SH3 domain does not (Table 2). This result is consistent with the five SH3 domains alignment in NADPH oxidase with a conserved sequence V59 seen in p40^{phox} and p67^{phox} C-terminal SH3 domains (Fig. 1). The data may also explain why both p40^{phox} and p67^{phox} C-terminal SH3 domains can bind to the same target of p47^{phox} proline-rich region (4, 5). Moreover, the data also suggest that the boundary site of p47^{phox} N-terminal SH3 domain may be located at L62 that exhibited distinct sequence compared to V59 in p40^{phox} and p67^{phox} C-terminal SH3 domain.

Determining the Boundary Sequence of the p67^{phox} C-Terminal SH3 Domain: Random-Directed Mutagenesis

To gain more details of mutations of these sites, we next performed random mutagenesis at positions P55, F58, V59 and E60. The results show that P55 to I55, G55, V55, W55, N55, E55, H55, and F55 resulting in the binding to p47^{phox} proline-rich region activity were completely abolished (Table 3). F58 to Tyr shows no effect of this binding, suggesting that aromatic stacking rather than hydrogen bonding is produced by this residue (Table 3). At V59 position, we gained seven different mutations to show that V59 can be replaced by F59, S59, G59, and I59, but can not be replaced by E59, N59 and L59 (Table 3). These data are consistent with the conformational preferences of the amino acids to favor β-strand (25, 26). A general conclusion at this point is that a various residues type can be substituted at V59 position are able to make compensatory tolerable β-sheet packing in SH3 domain.

TABLE 1

Various Boundary Site Mutants in the p67^{phox} C-Terminal SH3 Domain That Affect Interaction with the p47^{phox} Proline-Rich Region

Mutant	Tail sequence	Selection on SD medium		β-gal assay	
		−Trp −His −Ura	−Trp −His −Ura −Leu	Filter assay	Liquid assay
Wild type	I_{53}FPKVFVEDCAT$_{64}$	+	+	Blue	432.2 ± 46.32
(CCC)P55stop(TAA)	$I_{53}F_{54}$*	+	−	White	<20
(TTT)F58stop(TAA)	I_{53}FPKV_{57}*	+	−	White	<20
(GTT)V59stop(TAG)	I_{53}FPKVF_{58}*	+	−	White	<20
(GAA)E60stop(TAG)	I_{53}FPKVFV_{59}*	+	+	Blue	447.2 ± 40.15

Note. A series of p67^{phox} C-terminal SH3 domain mutants on pEG202 plasmid were tested for two-hybrid interaction with pJGA–p47^{phox} proline-rich in EGY48. β-Galactosidase unit is defined as the amount which hydrolyzes 1 μmol ONPG to *o*-nitrophenol per minute. Variations between replicates were less than 20%, and background activity was <20 U. *, stop codon; +, growth in SD medium; −, no growth.

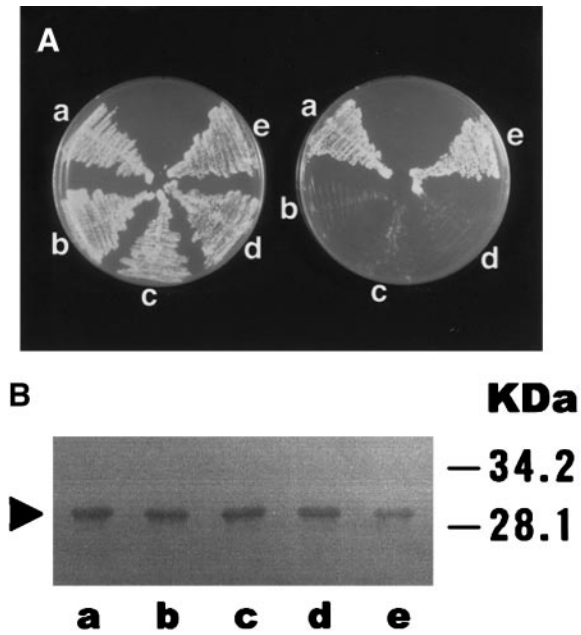

FIG. 2. (A) Yeast two-hybrid. Transactivation of *LEU2* reporter gene transcription in yeast coexpressing p67^{phox}/LexA binding domain and p47^{phox}/B42 activation domain fusion proteins. EGY48 yeast were cotransformed with pSH18-34, pEG202 expressing p67^{phox}/LexA binding domain fusion proteins, and pJG4-5 expressing p47^{phox}/B42 activation domain fusion proteins as described under Materials and Methods. Transformed yeast were streaked on left) galactose TRP- URA- HIS-; right) galactose TRP- URA- HIS- LEU-. Yeasts were cotransformed with p67^{phox} C-terminal SH3 domain: (a) wild type, (b) P55stop, (c) F58stop, (d) V59stop, and (e) E60stop and p47^{phox} proline-rich region (347–390). (B) Western blot. Expression of p67^{phox} C-terminal SH3/LexA binding domain fusion proteins in yeast. EGY48 cotransformed with pEG202 and pJG4-5 plasmids expressing p67^{phox} C-terminal SH3/LexA binding domain fusion proteins were pelleted and extracted with SDS–PAGE buffer as described under Materials and Methods. Lanes: (a) wild type, (b) P55stop, (c) F58stop, (d) V59stop, and (e) E60stop. The position of p67^{phox} C-terminal SH3/LexA fusion protein is indicated by the arrow. The molecular marker shown on the gel as indicated.

Specificity of the p67^{phox} C-Terminal SH3 Domain Wild Type and V59L Mutant in NADPH Oxidase

Based on the sequence alignment, either V59 or L59, seen in all SH3 domains, we observe that p67^{phox} C-terminal SH3 domain and p40^{phox} SH3 domain contained Val residue at position 59, whereas the other three SH3 domains contained Leu at an equivalent position of NADPH oxidase (Fig. 1). As shown in Table 3, we noticed that V59 residue particularly could not be replaced by Leu. This raises a possibility that V59L mutant in p67^{phox} C-terminal SH3 domain may lose its natural binding to p47^{phox} proline-rich target and switch its specificity for binding to other proline-rich targets (such as, p67^{phox} and p22^{phox} proline-rich region) in the NADPH oxidase. We therefore examined whether V59L mutant switched its binding activity to other proline-rich targets. Unfortunately, the results show that V59L mutant did not switch to bind to either p67^{phox} or p22^{phox} proline-rich targets, while wild type is still specific to its p47^{phox} proline-rich natural target (Table 4). This would suggest that V59 substituted alone is not sufficient to confer specificity. To avoid the error during construction, we also performed site-directed mutagenesis to revert V59L mutant back to wild-type V59. As expected, the revertant restored its binding activity, suggesting V59 residue is crucial and specific for binding (Table 4). All constructs were ver-

TABLE 2

Various Boundary Site Mutants in Different SH3 Domains That Affect Binding Activity with the Proline-Rich Region

SH3 domain	Tail mutant alignment	Binding activity
p67^{phox} C-terminal SH3	VGIFPKVF$_{58}$*	−
	VGIFPKVFV$_{59}$*	+
p40^{phox} SH3	TGIFPLSF$_{58}$*	−
	TGIFPLSFV$_{59}$*	+
p47^{phox} N-terminal SH3	RGWIPASF$_{58}$*	−
	RGWIPASFL$_{59}$*	−
	RGWIPASFLEPL$_{62}$*	+

Note. A series of SH3 domain mutants on pEG202 plasmid were tested for two-hybrid interaction. *, stop codon; +, positive interaction between domains tested; −, no interaction observed.

TABLE 3

Mutations in the p67^{phox} C-Terminal SH3 Domain That Affect Binding to the p47^{phox} Proline-Rich Region

Mutant		Selection on SD medium −Trp −His −Ura	Selection on SD medium −Trp −His −Ura −Leu	β-gal assay Filter assay
Wild type	IFPKVFVEDC	+	+	Blue
P55I	--I-------	+	−	White
P55G	--G-------	+	−	White
P55V	--V-------	+	−	White
P55W	--W-------	+	−	White
P55N	--N-------	+	−	White
P55E	--E-------	+	−	White
P55H	--H-------	+	−	White
P55F	--F-------	+	−	White
F58Y	-----Y----	+	+	Blue
V59F	------F---	+	+	Blue
V59S	------S---	+	+	Blue
V59G	------G---	+	+	Blue
V59I	------I---	+	+	Blue
V59E	------E---	+	−	White
V59N	------N---	+	−	White
V59L[a]	------L---	+	−	White

Note. A series of p67^{phox} C-terminal SH3 domain mutants on pEG202 plasmid were tested for two-hybrid interaction. +, growth in SD medium; −, not growth.

[a] It is noted that mutant V59L results in the loss of binding activity.

TABLE 4

Comparisons of Specificity of Interactions in the $p67^{phox}$ C-Terminal SH3 Domain, $p47^{phox}$ N-Terminal SH3 Domain, and $p40^{phox}$ SH3 Domain with the Proline-Rich Region

		Selection on SD medium		β-gal assay
BD	AD	−Trp −His −Ura	−Trp −His −Ura −Leu	Filter assay
$p67^{phox}$ C-SH3	Vector alone	+	−	White
$p47^{phox}$ N-SH3	Vector alone	+	−	White
$p40^{phox}$ SH3	Vector alone	+	−	White
$p67^{phox}$ C-SH3	$p47^{phox}_{proline\ rich}$	+	+	Blue
$p67^{phox}$ C-SH3	$P67^{phox}_{proline\ rich}$	+	−	White
$p67^{phox}$ C-SH3	$P22^{phox}_{proline\ rich}$	+	−	White
$p67^{phox}$ C-SH3 V59L	$P67^{phox}_{proline\ rich}$	+	−	White
$p67^{phox}$ C-SH3 V59L	$P22^{phox}_{proline\ rich}$	+	−	White
*$p67^{phox}$ C-SH3 ($V_{59} \rightarrow L \rightarrow V$)	$p47^{phox}_{proline\ rich}$	+	+	Blue
*$p67^{phox}$ C-SH3 ($V_{59} \rightarrow L \rightarrow V$)	$P67^{phox}_{proline\ rich}$	+	−	White
*$p67^{phox}$ C-SH3 ($V_{59} \rightarrow L \rightarrow V$)	$P22^{phox}_{proline\ rich}$	+	−	White
$p47^{phox}$ N-SH3	$P22^{phox}_{proline\ rich}$	+	+	Blue
$p40^{phox}$ SH3	$p47^{phox}_{proline\ rich}$	+	+	Blue

Note. A series of SH3 domains on pEG202 plasmid were tested for two-hybrid interaction with different prolin-rich regions. * indicates revertant; +, growth in SD medium; and −, no growth. BD, binding domain; AD, activation domain.

ified by sequencing and they expressed equal fusion protein levels by Western blot (data not shown).

Molecular Modeling of $p67^{phox}$ SH3–Ligand Complexes

A structural drawing of the $p67^{phox}$ C-terminal SH3 domain is based on the *c-src* SH3 domain X-ray crystal structure. The strands comprising the two antiparallel β-sheets of three and two β-strands are labeled βa–e. The side chains of conserved residues involved in target proline-rich peptide binding are shown (Fig. 3). It is clear that SH3 domain deletes V59 resulting in the missing of βe strand seen in the SH3 domain, which suggests the involvement of V59 in the βe (Fig. 3C). It is speculated that in this situation $p67^{phox}$ C-terminal SH3 domain may be not good enough to maintain its tertiary structure for binding to $p47^{phox}$ proline-rich region. Recently, V59 in different SH3 domains has been suggested to take part in the hydrophobic core of SH3 domain (19, 27, 28). For comparison, our results also refine the traditional view of X-ray crystallography structure of SH3 domain, as well as the suggestion that V59 is not only the hydrophobic core and also the boundary site to form βe strand in $p67^{phox}$ C-terminal SH3 domain.

CONCLUSION

These data suggest that V59 provides not only the boundary site, but also the critical site for maintaining the βe portion in the β-barrel structure of the $p67^{phox}$ C-terminal SH3 domain. Furthermore, our data show that V59 particularly could not be replaced by Leu (Tables 3 and 4), suggesting that this residue may

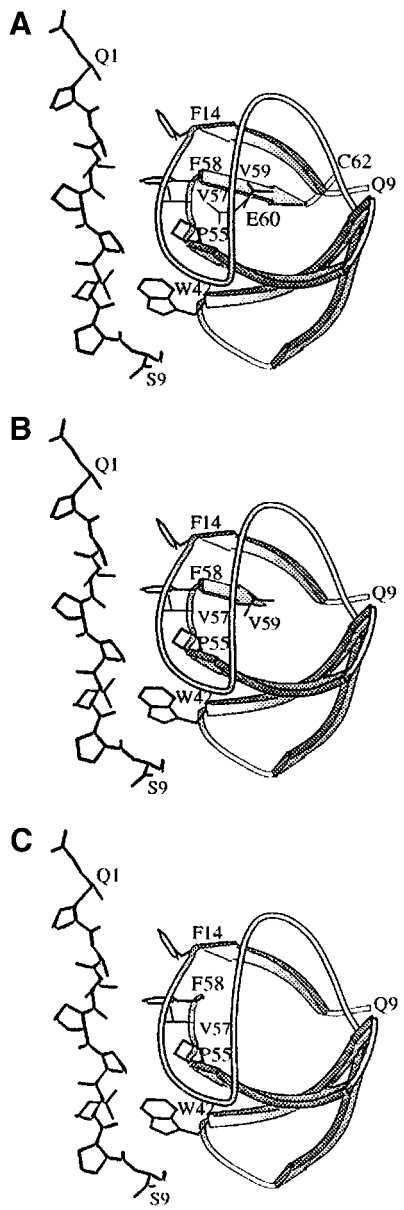

FIG. 3. A structural drawing of the $p67^{phox}$ C-terminal SH3 domain based on the X-ray crystal structure of the *c-src* SH3 domain structure as a template bound to the $p47^{phox}$ proline-rich (QPAVPPRPS) sequence. The strands comprising the two antiparallel β-sheets of three and two strands are labeled βa–e. The side chains of conserved residues involved in target proline-rich peptide binding are shown. (A) Wild type. (B) Minimal size of SH3. Note that V59 is the boundary sequence. (C) Without βe. Graphics were produced using Molscript (22).

affect the specificity of SH3 interactions in phagocyte NADPH oxidase.

ACKNOWLEDGMENTS

This work was supported by NSC 89-2745-P-037-001 (Taiwan, Republic of China), NSC 90-2314-B-037-107 to S.-L.H., and NSC 87-2314-B-037-062 to Y.-R.H.

REFERENCES

1. Umeki, S. (1994) *Ann. Hematol.* **68,** 267–277.
2. Rotrosen, D., Yeung, C. L., Leto, T. L., Malech, H. L., and Kwong, C. H. (1992) *Science* **256,** 1459–1462.
3. Heyworth, P. G., Bohl, B. P., Bokoch, G. M., and Curnutte, J. T. (1994) *J. Biol. Chem.* **269,** 30749–30752.
4. Fuchs, A., Dagher, M. C., and Vignais, P. V. (1995) *J. Biol. Chem.* **270,** 5695–5697.
5. Fuchs, A., Dagher, M. C., Faure, J., and Vignais, P. V. (1996) *Biochim. Biophys. Acta* **1312,** 39–47.
6. Leto, T. L., Garrett, M. C., Fujii, H., and Nunoi, H. (1991) *J. Biol. Chem.* **266,** 19812–19818.
7. Leto, T. L., Adams, A. G., and de Mendez, I. (1994) *Proc. Natl. Acad. Sci. USA* **91,** 10650–10655.
8. McPhail, L. C. (1994) *J. Exp. Med.* **180,** 2011–2015.
9. Park, J. W., Ma, M., Ruedi, J. M., Smith, R. M., and Babior, B. M. (1992) *J. Biol. Chem.* **267,** 17327–17332.
10. Iyer, S. S., Pearson, D. W., Nauseef, W. M., and Clark, R. A. (1994) *J. Biol. Chem.* **269,** 22405–22411.
11. Finan, P., Shimizu, Y., Gout, I., Hsuan, J., Truong, O., Butcher, C., Bennett, P., Waterfield, M. D., and Kellie, S. (1994) *J. Biol. Chem.* **269,** 13752–13755.
12. Leusen, J. H. W., Fluiter, K., Hilarius, P. M., Veroeven, A. J., and Bolscher, G. J. M. (1995) *J. Biol. Chem.* **270,** 11216–11221.
13. Sumimoto, H., Kage, Y., Nunoi, H., Sasaki, H., Nose, T., Fukumaki, Y., Ohno, M., Minakami, S., and Takeshige, K. (1994) *Proc. Natl. Acad. Sci. USA* **91,** 5345–5349.
14. Hong, Y. R., Han, L., Huang, J., and Kleinberg, M. E., and Malech, H. L. (1996) *Kaohsiung J. Med. Sci.* **12,** 301–305.
15. Leto, T. L., Lomax, K. J., Volpp, B. D., Nunoi, H., Sechler, J. M. G., Nauseef, W. M., Clark, R. A., Gallin, J. I., and Malech, H. L. (1990) *Science* **248,** 727–730.
16. Musacchio, A., Wilmanns, M., and Saraste, M. (1994) *Prog. Biophys. Mol. Biol.* **61,** 283–297.
17. Finan, P., Koga, H., Zvelebil, M. J., Waterfield, M. D., and Kellie, S. (1996) *J. Mol. Biol.* **261,** 173–180.
18. Maxwell, K. L., and Davidson, A. R. (1998) *Biochemistry* **37,** 16172–16182.
19. Cordier, F., Wang, C., Grzesiek, S., and Nicholson, L. K. (2000) *J. Mol. Biol.* **304,** 497–505.
20. Golemis, E. A., Gyuris, J., and Brent, R. (1994) *in* Current Protocols in Molecular Biology, Supplement 27 (Ausubel, F. M., Ed.), pp. 13.14.1–13.14.17, Wiley, New York.
21. Mendelsohn, A. R., and Brent, R. (1994) *Curr. Opin. Biotechnol.* **5,** 482–486.
22. Kleinberg, M. E., Malech, H. L., Mital, D. A., and Leto, T. L. (1994) *Biochemistry* **33,** 2490–2495.
23. Brunger, A. T. (1992) XPLOR 3.1: A System for Crystallography and NMR, Yale Univ., New Haven, CT.
24. Kraulis, P. J. (1991) *J. Appl. Crystallogr.* **24,** 946–950.
25. Williams, R. W., Chang, A., Juretic, D., and Loughran, S. (1987) *Biochim. Biophys. Acta* **916,** 200–204.
26. Wilmot, C. M., and Thornton, J. M. (1988) *J. Mol. Biol.* **203,** 221–232.
27. Larson, S. M., Di Nardo, A. A., and Davidson, A. R. (2000) *J. Mol. Biol.* **303,** 433–446.
28. Grantcharova, V. P., and Baker, D. (2001) *J. Mol. Biol.* **306,** 555–563.